Time-series for Causal Inference Method in Environmental Research

Anonymous submission

Abstract

Many environmental studies aim to analyze data with spatial and time structures. This becomes both a blessing and a curse for causal inference. On one side, causality cannot be inferred without time. On the other hand, the time and space components introduce greater complexity in the data structures, making many existing statistical methods for causal inference inapplicable. We present a concise framework for estimating causal effects of time-varying exposures from single-unit time series under an observational studies setting. We define duration-t_0 estimands and model assignment with time-varying propensity scores $p_t(1 \mid \mathcal{F}_t)$ that condition on full history to address feedback, carryover, and seasonality. We derive a step-by-step stabilized IPW estimator with window weights and conservative Wald inference via a martingale variance bound. Under correct specification, using *estimated* propensity scores yields a consistent estimator whose asymptotic variance is no larger than the oracle known-PS IPW, delivering a practical efficiency gain. Simulations varying series length, intervention duration, and assignment mechanisms, plus a synthetic California $PM_{2.5}$ case study, illustrate bias, overlap diagnostics, and uncertainty quantification.

1 Introduction

Understanding how environmental exposures influence health outcomes over time is a central question in public health. Researchers often rely on time-series data, which track exposures such as air pollution or temperature alongside daily health outcomes. In environmental research, many people were aiming at study the effects of treatment using time-series data. The temporal ordering of exposures and outcomes makes causal inference possible, yet dependencies across time, lagged effects, and time-varying confounding pose substantial challenges. As Rune Christiansen and Peters (2022) observe, all data arise in space and time, and leveraging this structure can strengthen statistical modeling. In this paper, we focus on environmental applications, emphasizing methods for estimating the causal effects of time-varying exposures using time-series data.

Historically, causal inference with time-series data has received less attention, largely because of the technical challenges it presents. Unlike cross-sectional studies, time-series often involve a single unit repeatedly observed, where temporal dependence, lag effects, and time-varying confounding complicate identification and limit the use of standard estimands. In environmental epidemiology, researchers have long relied on regression-based methods to address these questions. Log-linear regression models are widely applied to estimate associations between exposures, such as air pollution, and health outcomes (Peng and Dominici 2008; Dominici et al. 2006). Case-crossover designs provide another popular strategy, comparing exposure levels at the time of an event to those at control times (Di et al. 2017; Shahn, Hernán, and Robins 2023; Lu and Zeger 2007). These conventional approaches are useful for adjusting confounding and quantifying associations, but they often lack a formal causal interpretation and can obscure the assumptions underlying identification. Causal inference methods share the same objective of reducing bias but go further by offering a structured framework to define potential outcomes, specify target populations, articulate causal estimands of interest, and separate the design from the analysis. This perspective not only clarifies the assumptions required for valid inference but also highlights potential sources of bias that conventional regression-based approaches may overlook.

These considerations motivate a framework that links time-series structure to causal inference. Bojinov and Shephard (2019) extend potential outcomes to single-unit time series, define unit-level causal estimands (including lag effects), and show how to conduct randomization-based inference with minimal assumptions. Their work is rooted in experimental settings, where treatment assignment is randomized and propensity scores are known by design. In contrast, our focus is on observational studies in environmental research, where exposures such as air pollution or temperature are not randomized and propensity scores must be estimated. This observational setting raises additional challenges for identification and inference, but it also reflects the realities of most environmental applications. Building on these ideas, the objective of this article is to provide a detailed, step-by-step tutorial on formulating causal estimands, designing treatment assignment strategies, estimating effects, and quantifying uncertainty for time-series data in observational environmental studies.

2 Background

Conventional regression methods have long served as foundational tools in environmental epidemiology for estimating

associations between environmental exposures and health outcomes. One widely used approach is the overdispersed Poisson regression model, often referred to as a log-linear model, which estimates the relative rate of adverse health events associated with short-term changes in environmental exposures such as air pollution or heat. These models incorporate smooth functions of calendar time and meteorological covariates to control for confounding by long-term trends and seasonality (Dominici et al. 2006; Peng and Dominici 2008). In parallel, the case-crossover design has been increasingly adopted for its intuitive appeal and capacity to eliminate time-invariant confounders by design. Under this approach, each subject serves as their own control by comparing exposure levels at the time of the event to those at referent control periods. This strategy has been shown to be formally equivalent to certain time-series methods under specific assumptions and has gained traction in large-scale studies of air pollution and mortality (Di et al. 2017; Lu and Zeger 2007; Shahn, Hernán, and Robins 2023). Both regression-based and case-crossover designs can be flexibly adapted to incorporate multiple lags, distributed lag structures, and hierarchical pooling across spatial units, forming the empirical backbone of many multi-site environmental health studies in the last two decades.

While traditional regression-based approaches focus on controlling for confounding through model specification, the modern causal inference framework offers a structured approach to defining causal effects and identifying assumptions. In time-series and spatio-temporal environmental studies, this framework is crucial for understanding the impact of exposures that evolve dynamically over time and vary across locations.

Causal Inference Methods

The goals of causal inference in environmental time-series studies align closely with those of conventional regression-based methods: both seek to adjust for confounding and quantify the relationship between exposures and outcomes. However, causal inference introduces a formal framework to articulate, identify, and estimate causal effects, bringing conceptual clarity and methodological rigor. This framework emphasizes four key components: (i) the explicit definition of potential outcomes and target populations; (ii) formal specification of the causal estimand of interest; (iii) clear separation of study design from analysis; and (iv) structured evaluation of identification assumptions and potential biases. In the context of environmental epidemiology, the temporal dimension of exposure and outcome processes necessitates specialized adaptations of causal inference methodology. Below, we review key developments in this area, beginning with the potential outcomes framework and extending to the use of propensity scores in time-series settings.

Potential Outcomes Framework The potential outcomes framework provides a foundational language for causal inference, allowing researchers to define causal effects with precision and to formalize assumptions necessary for their identification. For a unit i at time t, the potential outcome $Y_{it}(w_{1:t})$ represents the health outcome that would be observed if the exposure history up to time t followed the path $w_{1:t} = (w_1, \ldots, w_t)$. Only one such potential outcome is realized for each unit—corresponding to the observed exposure trajectory $W_{1:t}$—so causal effects must be inferred by contrasting observed outcomes with counterfactuals.

A basic causal estimand is the difference between potential outcomes under two exposure scenarios:

$$\tau_{it} = Y_{it}(w_{1:t}) - Y_{it}(w'_{1:t}),$$

where $w_{1:t}$ and $w'_{1:t}$ are alternative histories of the exposure process. More complex estimands may average these differences across units or focus on marginal contrasts, cumulative effects, or duration-specific impacts.

Identification of causal effects from observed data requires assumptions such as:

- **Consistency**: The observed outcome equals the potential outcome under the observed exposure history.
- **No unmeasured confounding**: All variables that jointly influence treatment assignment and the outcome are observed.
- **Temporal ordering**: Treatments at time t are assigned based only on past and present information.

These assumptions are often challenging in spatio-temporal environmental settings, where exposures and confounders evolve dynamically, and where individual units may interact or be subject to shared environmental shocks.

Time-Series Experimental and Observational Studies: Propensity Scores Recent extensions of the potential outcomes framework to time-series data have introduced innovative strategies for defining causal estimands and estimating effects in both experimental and observational contexts. Bojinov and Shephard (2019) formalize causal inference in time-series experiments by considering interventions over time and deriving exact randomization-based tests. Their work addresses key challenges such as serial dependence in outcomes and treatments, and emphasizes the importance of defining estimands that reflect the sequential nature of interventions.

In observational studies, dynamic treatment assignment further complicates identification. Propensity scores—originally developed for cross-sectional data—have been generalized to time-varying settings, where the probability of receiving treatment at time t depends on a filtration $\mathcal{F}_t$ that encodes the observed history up to t. Specifically, the time-varying propensity score is defined as:

$$p_t = \Pr(W_t = 1 \mid \mathcal{F}_t),$$

where $\mathcal{F}_t = \{C_{1:t}, W_{1:(t-1)}, Y_{1:(t-1)}\}$ includes past covariates, treatments, and outcomes. Weighting or stratifying on these propensity scores can mitigate confounding and facilitate unbiased estimation of causal effects, even under complex temporal dynamics.

Wu et al. (2024) apply this perspective to evaluate the effectiveness of stochastic interventions in public health. By modeling heat alerts as probabilistic functions of weather forecasts, they estimate the causal effects of such alerts on mortality and hospital admissions. Their work demonstrates

the feasibility of using time-varying propensity scores to evaluate policies that are not deterministic, and that vary both across space and over time.

Papadogeorgou et al. (2022) extend the framework further to accommodate spatial correlation and interference. Their Bayesian model for causal inference with spatio-temporal data incorporates random effects and allows for dynamic treatment regimes and heterogeneous treatment effects across regions. This approach is particularly well-suited for environmental studies, where exposures and outcomes may be spatially clustered, and where units (e.g., counties or cities) may influence one another through shared infrastructure or population mobility.

Together, these developments underscore the adaptability of causal inference methods to spatio-temporal data. By explicitly modeling exposure dynamics, temporal confounding, and spatial heterogeneity, modern approaches provide a principled foundation for causal claims in environmental research. As we discuss in the following sections, these frameworks not only clarify conceptual targets but also guide the construction of estimators and the interpretation of policy-relevant effects.

3 Motivational Example and Notation

As a motivating example, we consider the causal effect of short-term exposure to ambient fine particulate matter ($PM_{2.5}$) on daily mortality counts across California counties. Our focus is on quantifying the effect of exposure persistence over a fixed temporal window on health outcomes, such as estimating the effect of elevated $PM_{2.5}$ levels sustained for $t_0 = 3$ consecutive days.

To facilitate methodological development and reproducibility, we consider both a simulation framework and an application study that mirrors key challenges in air pollution studies, including: time-varying exposure, lagged effects and time-varying confounding. This setting motivates the development and evaluation of time-series estimators that can recover well-defined causal effects under dynamic treatment regimes and observational confounding.

Problem Setup and Notation

We consider a single-unit time series of length T, where at each time point $t \in \{1, \ldots, T\}$, we observe:

- a binary exposure $W_t \in \{0, 1\}$, indicating high $PM_{2.5}$ on day t,
- a vector of covariates C_t (e.g., temperature, humidity, calendar indicators),
- an outcome $Y_t \in \mathbb{R}$, representing the daily mortality count (or rate),
- a filtration $\mathcal{F}_t = \{C_{1:t}, W_{1:(t-1)}, Y_{1:(t-1)}\}$, containing all past information observed prior to treatment assignment at time t.

Our goal is to estimate the **causal effect** of a binary treatment regime $\delta_{t-t_0+1:t} \in \{0, 1\}^{t_0}$ applied over a window of length t_0. At time t, we define the following potential outcomes–based estimand:

$$\tau_t(\delta_{t-t_0+1:t}) = \mathbb{E}\left[Y_t\big(W^{\text{obs}}_{1:t-t_0}, \delta_{t-t_0+1:t}\big) - Y_t\big(W^{\text{obs}}_{1:t-t_0}, \delta'_{t-t_0+1:t}\big) \,\middle|\, \mathcal{F}_{t-t_0}\right],$$

where:

- $W^{\text{obs}}_{1:t-t_0}$: the observed treatment trajectory prior to the intervention window,
- $\delta_{t-t_0+1:t}$: the active exposure regime of interest (e.g., 3 days of high $PM_{2.5}$),
- $\delta'_{t-t_0+1:t}$: a reference regime (e.g., 3 days of low $PM_{2.5}$),
- $\mathcal{F}_{t-t_0}$: sigma-algebra containing observed history up to time $t - t_0$.

This estimand captures the time-specific causal effect of replacing the most recent t_0 treatments with a specified regime, conditioning on past history. By varying δ, we can evaluate dynamic, lagged, or even cumulative effects of treatment exposure over time. To estimate this quantity from observational data, we require several assumptions common to longitudinal causal inference:

- **Sequential ignorability**: No unmeasured confounders given $\mathcal{F}_t$.
- **Positivity**: All treatment regimes under consideration must occur with positive probability given past history.
- **Consistency**: The observed result under the observed treatment is equal to the potential outcome under that treatment.
- **No interference**: Exposure of one unit does not affect the outcome of another (naturally satisfied in single-unit time series).

Time-varying Propensity Score Models

Following recommendations by (Bojinov, Rambachan, and Shephard 2021), we estimate the time-varying propensity scores $p_t = \Pr(W_t = 1 \mid \mathcal{F}_t)$ using both:

- **Logistic regression (GLM)** with a correctly specified functional form and logit link. Specificly, we assume the logistic regression model is correctly specified as:

$$\log\left(\frac{p_t}{1 - p_t}\right) = \beta_0 + \beta_1 W_{t-1} + \beta_2 \bar{X}_t;$$

- **Super Learner** (Van der Laan, Polley, and Hubbard 2007), an ensemble learning method combining generalized additive models, multivariate adaptive regression splines, support vector machines, random forests, and parametric generalized linear models, as recommended by Kennedy (2019).

How the Filtration Controls Time-Varying Confounding

We encode the observable history by the filtration $\mathcal{F}_t = \{C_{1:t}, W_{1:(t-1)}, Y_{1:(t-1)}\}$. Conditioning on $\mathcal{F}_t$ in the time-varying propensity score

$$p_t(1 \mid \mathcal{F}_t) = \Pr(W_t = 1 \mid C_{1:t}, W_{1:(t-1)}, Y_{1:(t-1)})$$

accounts for (i) past treatments $W_{1:(t-1)}$ (carryover), (ii) past outcomes $Y_{1:(t-1)}$ (feedback), and (iii) time-varying covariates $C_{1:t}$ (weather, seasonality, etc.), thereby addressing key sources of time-varying confounding. We invoke standard longitudinal assumptions: (i) **Sequential ignorability** $W_t \perp\!\!\!\perp Y_t(w_{1:t}) \mid \mathcal{F}_t$; (ii) **Positivity**: $0 < \epsilon \le p_t(1 \mid \mathcal{F}_t) \le 1 - \epsilon < 1$; (iii) **Consistency**; (iv) **No interference** (single-unit series). Residual bias may remain if there are unmeasured *time-varying* confounders, model misspecification of p_t, complex feedback not captured by $\mathcal{F}_t$, or practical violations of positivity (near-deterministic exposure). We discuss robust variance estimation and diagnostics in Appendix.

4 Asymptotic Properties and Relative Efficiency

We study large-sample properties of the duration-t_0 IPW estimators when propensity scores are known (oracle) versus estimated from data. Let

$$u_{t,0} = \left(\tfrac{\mathbb{1}\{W_t=1\}}{p_t(1)} - \tfrac{\mathbb{1}\{W_t=0\}}{p_t(0)} \right) Y_t(w^{\text{obs}}_{1:t})$$

be the period-t influence term for the contemporaneous effect ($t_0 = 0$). Under bounded outcomes and randomized (or ignorable) assignment conditional on $\mathcal{F}_t$, $\{u_{t,0}, \mathcal{F}_{t-1}\}$ is a martingale difference array. By the martingale CLT (Heyde and Hall 1980), $\sqrt{T}\left(\widehat{\bar{\tau}} - \bar{\tau}\right) \xrightarrow{d} \mathcal{N}(0, \eta^2)$, with conditional variance $\eta^2 = \lim_{T\to\infty} T^{-1} \sum_{t=1}^{T} \operatorname{var}^R(u_{t,0} \mid \mathcal{F}_{t-1})$. A conservative feasible bound is

$$\widehat{\sigma}^2_T = \frac{1}{T}\sum_{t=1}^{T} \widehat{\sigma}^2_t, \qquad \widehat{\sigma}^2_t = \frac{Y_t(w^{\text{obs}}_{1:t})^2}{p_t(1)\, p_t(0)}. \tag{1}$$

A 95% Wald interval is then $\widehat{\bar{\tau}} \pm 1.96\sqrt{\widehat{\sigma}^2_T/T}$, which remains valid under weak nonstationarity provided $p_t(1) \in (0,1)$. Let $\widehat{p}_t(1 \mid \mathcal{F}_t)$ be a correctly specified and consistent estimate of $p_t(1 \mid \mathcal{F}_t)$. Consider the IPW estimator that replaces p_t by $\widehat{p}_t$ in the window weight.

Theorem. *(Asymptotic properties with estimated propensity scores) Under correct specification of the propensity score model and regularity conditions, the IPW estimator with estimated propensity socre is: (i) asymptotically consistent: $\hat{\tau}^{IPW} \xrightarrow{p} \tau$; (ii) has asymptotic normality and variance that is no larger than the asymptotic variance of the same estimator using the true propensity score.*

Intuition. Estimating p_t introduces an extra score term that projects part of the variability onto the propensity model's tangent space, yielding a variance reduction (an "estimated-nuisance" efficiency gain). A full proof is deferred to Appendix. For finite samples we recommend: (i) the conservative martingale bound in (1); (ii) as a sensitivity check, a heteroskedasticity–autocorrelation robust (HAC/Newey–West) variance for the influence sequence when overlap is good; (iii) trimming or stabilized weights when near-violations of positivity are detected. We report both point estimates and bound-based intervals in Section 6 and Section 7.

5 Step-by-step Estimation of ATE

Given an estimated or known propensity score sequence $\{p_t\}_{t=1}^{T}$, we estimate the duration-t_0 causal effect using the stabilized inverse probability weighting (IPW) estimator.

Step 1: Compute individual weights. For each time t, we define the cumulative IPW across a window of length t_0 as:

$$w_t(t_0) = \prod_{s=t}^{t+t_0} \frac{1}{p_s(W_s \mid \mathcal{F}_s)}.$$

Step 2: Compute window-specific IPW outcomes. Let $Y^{\text{obs}}_{t+t_0}$ denote the observed outcome at the end of the window. The weighted outcome is:

$$\hat{\tau}^{\text{IPW}}_t(t_0) = w_t(t_0) \cdot Y^{\text{obs}}_{t+t_0}.$$

Step 3: Aggregate over time. The overall ATE estimator is obtained by averaging across valid windows:

$$\hat{\text{ATE}} = \frac{1}{T - t_0} \sum_{t=1}^{T-t_0} \hat{\tau}^{\text{IPW}}_t(t_0).$$

Error decomposition under the null. To facilitate inference, we consider the **sharp null of no average temporal causal effect at lag zero**, stated as:

$$H_0 : \bar{\tau}_0 = 0,$$

which implies that the contemporaneous treatment has no average effect on the outcome over time. This is a relaxation of the stronger sharp null $Y_t(w_{1:t}) = Y_t(w'_{1:t})$ for all treatment paths, and is commonly referred to as the Neyman null in the non-time-series setting.

Under H_0, we define the time-specific estimation error for the contemporaneous IPW estimator as:

$$u_{t,0} = \left(\frac{1_{W_t=1}}{p_t(1)} - \frac{1_{W_t=0}}{p_t(0)} \right) Y_t(w^{\text{obs}}_{1:t}).$$

This quantity measures the deviation of the IPW estimator from its (null) expectation at each time t. Under the assumption of random assignment of W_t and bounded outcomes, the sequence $\{u_{t,0}, \mathcal{F}_{T,t-1}\}_{t=1}^{T}$ forms a martingale difference array. This property underlies the validity of the central limit theorem in the following step.

Step 4: Estimate standard error via martingale variance bound. Under the sharp null of no average temporal causal effect, and assuming the treatment path is randomized, the estimation error

$$u_{t,0} = \left(\frac{1_{W_t=1}}{p_t(1)} - \frac{1_{W_t=0}}{p_t(0)} \right) Y_t(w^{\text{obs}}_{1:t})$$

forms a martingale difference array. By Theorem 3 in (Heyde and Hall 1980), the normalized sum satisfies a central limit theorem:

$$\sqrt{T}\left(\hat{\bar{\tau}} - \bar{\tau}\right) \xrightarrow{d} \mathcal{N}(0, \eta^2),$$

where

$$\hat{\eta}^2_T = \frac{1}{T}\sum_{t=1}^{T} \operatorname{var}^R(u_{t,0} \mid \mathcal{F}_{T,t-1})$$

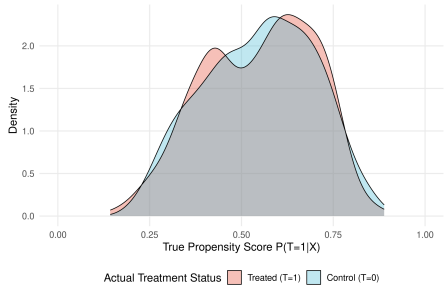

Figure 1: Propensity Score Distribution: TRUE PS

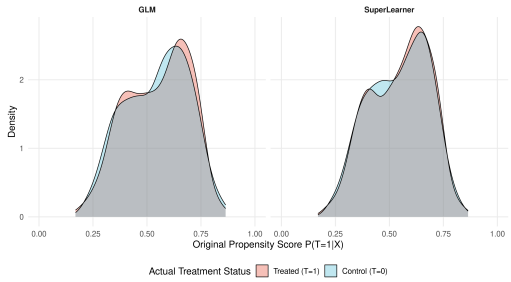

Figure 2: Propensity Score Distribution: GLM vs SuperLearner

is the conditional variance of the influence function estimator, which may depend on unobserved counterfactuals.

To ensure valid inference under minimal assumptions, we instead use an upper bound estimator

$$\widehat{\sigma}_T^2 = \frac{1}{T}\sum_{t=1}^{T}\hat{\sigma}_t^2,$$

where $\hat{\sigma}_t^2$ is a conservative variance bound for $u_{t,0}$ computed via:

$$\hat{\sigma}_t^2 = \frac{Y_t(w_{1:t}^{\text{obs}})^2}{p_t(1)p_t(0)}.$$

Step 5: Construct asymptotically valid 95% confidence interval. We construct a Wald-type confidence interval using the bound-adjusted variance:

$$\hat{\bar{\tau}} \pm 1.96 \cdot \sqrt{\frac{1}{T}\sum_{t=1}^{T}\hat{\sigma}_t^2}.$$

This interval is conservative and remains asymptotically valid under weak conditions, including nonstationarity in the outcome-generating process, provided $p_t(1) \in (0,1)$ and the outcome remains bounded.

6 Simulation Study

Data Generating Mechanism

We study finite-sample properties of the proposed estimators via simulation studies on a single time series, in which we vary: (i) the length of the time series T; (ii) the duration of interventions t_0; and (iii) the assignment mechanisms of the treatment $p_t(W_t = 1 \mid \mathcal{F}_t)$.

To reflect the nature of treatment assignment in our motivating example, we generate the treatment W_t under a nearly non-overlapping setting. Specifically, for each time point $t = 1, \ldots, T$, we generate:

$$X_t = (X_{1,t}, X_{2,t}, X_{3,t}, X_{4,t}, X_{5,t}) \sim \mathcal{N}(0, I_5),$$

$$\bar{X}_t = \frac{1}{5}\sum_{j=1}^{5} X_{j,t}, \quad W_{t-1} = a_{\text{lag1}}[t],$$

$$p_t = \text{expit}\left\{\bar{X}_t - W_{t-1} + 0.5\right\}, \quad W_t \sim \text{Bernoulli}(p_t),$$

$$Y_t \sim \mathcal{N}(3W_t + 1W_{t-1} + \bar{X}_t, 1).$$

In the randomized setting, we generate covariates $X_t \sim \mathcal{N}(0, I_5)$ with mean $\bar{X}_t = \frac{1}{5}\sum_{j=1}^{5} X_{j,t}$, and assign treatment independently as $W_t \sim \text{Bernoulli}(0.5)$ with $W_0 = 0$, so that the true propensity scores are known by design ($p_t \equiv 0.5$). The outcome preserves a duration-1 effect, depending on both the contemporaneous and lagged treatments, $Y_t \sim \mathcal{N}(3W_t + W_{t-1} + \bar{X}_t, 1)$.

True Potential Outcomes and ATE

The conditional potential outcome mean is:

$$\mathbb{E}[Y_t(w_t, w_{t-1}) \mid \bar{X}_t] = 3w_t + 1w_{t-1} + \bar{X}_t.$$

Thus, the true contemporaneous ATE is:

$$\boxed{\text{ATE}_{\text{true}} = 3.}$$

Implementation of IPW Estimator

Given the fitted or true propensity scores $p_s(1 \mid \mathcal{F}_s)$, we define stabilized weights:

$$w_s = \frac{1}{p_s(W_s \mid \mathcal{F}_s)} = \begin{cases} 1/p_s(1 \mid \mathcal{F}_s), & \text{if } W_s = 1 \\ 1/p_s(0 \mid \mathcal{F}_s), & \text{if } W_s = 0 \end{cases}$$

and compute the cumulative weight: $W_t(t_0) = \prod_{s=t}^{t+t_0} w_s$.The estimator for each time t is:

$$\hat{\tau}_t^{\text{IPW}}(t_0) = W_t(t_0) \cdot Y_{t+t_0}^{\text{obs}}.$$

Average across time gives:

$$\hat{\text{ATE}} = \frac{1}{T - t_0}\sum_{t=1}^{T-t_0} \hat{\tau}_t^{\text{IPW}}(t_0).$$

Unbiasedness Justification

Since the observed outcome satisfies

$$Y_t^{\text{obs}} = W_t Y_t(1) + (1 - W_t)Y_t(0),$$

multiplying by $(-1)^{1-W_t}$ yields:

$$(-1)^{1-W_t} Y_t^{\text{obs}} = \begin{cases} Y_t(1), & \text{if } W_t = 1, \\ -Y_t(0), & \text{if } W_t = 0. \end{cases}$$

Thus, taking the expectation with respect to $\mathcal{F}_t$, we obtain:

$$\mathbb{E}\left[\frac{(-1)^{1-W_t} Y_t^{\text{obs}}}{\Pi_t}\,\middle|\,\mathcal{F}_t\right] = \mathbb{E}[Y_t(1) - Y_t(0)],$$

where $\Pi_t = \prod_{s=t}^{t+t_0} p_s(W_s \mid \mathcal{F}_s)$ is the joint probability of the observed treatment path.

Finally, applying a variance stabilization factor 2^{-t_0} (following Shephard & Bojinov (Bojinov and Shephard 2019)), we have the full Horvitz-Thompson estimator:

$$\boxed{\widehat{\tau}_{t_0} = \frac{1}{T - t_0} \sum_{t=t_0+1}^{T} \left(2^{-t_0} \frac{(-1)^{1-W_t} Y_t^{\text{obs}}}{\Pi_t} \right)}$$

Simulation results

Across $T \in \{200, 1000, 5000\}$ and lags $t_0 \in \{0, 1, 4, 9\}$ (500 replications), the IPW estimator recovers the truth: absolute bias is near zero when the PS is known or correctly specified (GLM), with MSE and CI length shrinking as T grows (Table 1). Super Learner shows higher small-sample bias/variance under randomization but approaches GLM as T increases. Coverage using the martingale-bound SE is conservative (often $\geq 95\%$), especially for larger t_0 where weights compound and variance increases. Overall, with adequate overlap, duration-t_0 effects are estimated reliably; correct PS modeling is more crucial than additional flexibility, and longer windows ($t_0 > 0$) trade bias control for wider intervals.

T	t_0	Metric	ps.true	glm.model	SL.model	PS0.5
200	0	abs bias ($\theta = 3$)	0.005	0.000	0.212	0.000
		mse	0.113	0.005	0.092	0.110
		Length	1.701	1.766	1.716	1.536
		coveragerate	98.600	100.000	99.600	97.400
200	1	abs bias ($\theta = 1$)	0.021	0.007	0.358	0.014
		mse	0.214	0.082	0.191	0.157
		Length	1.810	1.946	1.846	1.543
		coveragerate	94.600	100.000	98.800	94.800
200	4	abs bias ($\theta = 0$)	0.045	0.020	0.014	0.017
		mse	0.359	0.353	0.080	0.142
		Length	2.171	2.613	2.316	1.554
		coveragerate	92.800	96.400	99.800	96.400
200	9	abs bias ($\theta = 0$)	0.010	0.037	0.023	0.018
		mse	0.887	1.231	0.084	0.164
		Length	2.942	4.414	3.565	1.575
		coveragerate	94.400	96.400	99.800	95.600
1000	0	abs bias ($\theta = 3$)	0.001	0.001	0.099	0.000
		mse	0.028	0.001	0.025	0.021
		Length	0.760	0.766	0.762	0.688
		coveragerate	98.400	100.000	96.200	98.000
1000	1	abs bias ($\theta = 1$)	0.007	0.002	0.142	0.004
		mse	0.050	0.012	0.041	0.031
		Length	0.806	0.819	0.810	0.688
		coveragerate	92.600	100.000	95.400	94.200
1000	4	abs bias ($\theta = 0$)	0.002	0.001	0.001	0.005
		mse	0.078	0.047	0.027	0.030
		Length	0.961	0.998	0.971	0.690
		coveragerate	92.400	97.600	99.200	95.400
1000	9	abs bias ($\theta = 0$)	0.006	0.022	0.005	0.006
		mse	0.127	0.122	0.045	0.032
		Length	1.287	1.392	1.322	0.691
		coveragerate	92.600	95.200	98.800	95.000
5000	0	abs bias ($\theta = 3$)	0.005	0.000	0.051	0.002
		mse	0.005	0.000	0.008	0.004
		Length	0.340	0.340	0.340	0.307
		coveragerate	98.600	100.000	89.400	97.800
5000	1	abs bias ($\theta = 1$)	0.006	0.001	0.065	0.003
		mse	0.009	0.002	0.012	0.005
		Length	0.360	0.361	0.361	0.308
		coveragerate	93.600	100.000	87.800	97.600
5000	4	abs bias ($\theta = 0$)	0.005	0.004	0.003	0.002
		mse	0.014	0.009	0.007	0.005
		Length	0.429	0.432	0.430	0.308
		coveragerate	92.800	97.600	99.200	96.400
5000	9	abs bias ($\theta = 0$)	0.003	0.002	0.004	0.004
		mse	0.027	0.023	0.014	0.005
		Length	0.574	0.582	0.577	0.308
		coveragerate	93.200	94.600	97.600	96.600

Table 1: Randonmization Experiment's ATE (500 replications)

7 Application

To evaluate the performance of time-series methods for causal inference in environmental health, we constructed a synthetic application study that emulates the real-world challenge of estimating the short-term effects of air pollution on population mortality. Specifically, we focused on assessing the causal impact of ambient $PM_{2.5}$ exposure on daily mortality counts across all 58 counties in California over the period 2015–2019. Drawing from high-resolution $PM_{2.5}$ exposure estimates and incorporating realistic covariate structures, we simulated county-day mortality counts using a Poisson model with seasonal variation and a log-linear exposure-response relationship. To reflect practical epidemiological settings, we included potential confounders such as daily maximum temperature, precipitation, weekday effects, and federal holidays. A binary treatment indicator was derived using a regulatory threshold of $11\mu g/m^3$ for $PM_{2.5}$. Importantly, we accounted for lagged exposure effects and dynamic treatment assignment, allowing us to examine both contemporaneous and delayed associations. This synthetic setup allows for benchmarking causal estimators under known ground truth, while preserving key temporal and spatial complexities present in real-world data.

Data

Mortality Data. We simulated synthetic daily mortality counts (trend seen in Appendix B) for all 58 counties in California from Jan. 1, 2015 to Dec. 31, 2019. Synthetic daily mortality counts were generated for each county c and day t using a Poisson process that reflects seasonal mortality trends, geographic variation, and the effect of $PM_{2.5}$ exposure. Specifically, the observed count y_{ct} was drawn from:

$$y_{ct} \sim \text{Poisson}(\mu_{ct}) \tag{2}$$

where the expected mortality rate μ_{ct} was modeled as:

$$\mu_{ct} = \underbrace{\text{bline}_c}_{\text{baseline rate}} \times \underbrace{(1 + \alpha \cdot g(t))}_{\text{seasonal trend}} \times \underbrace{\exp(\beta_c x_{ct})}_{\text{exposure effect}} \tag{3}$$

with components defined as follows:

- bline_c: County-specific baseline mortality rate (calibrated from county-level population data)
- $\alpha = 0.1$: Amplitude of seasonal variation
- $g(t) = \cos\left(2\pi \cdot \frac{\text{doy}(t)}{365}\right)$: Annual periodicity function based on the day of year
- $\beta_c = \log(\text{RR}_c)$: Log-relative risk of exposure for c
- x_{ct}: Daily $PM_{2.5}$ concentration for county c at time t

This outcome model incorporates 3 essential elements:

1. **Geographic heterogeneity**, captured through county-specific baseline rates (bline_c) and exposure-response coefficients (β_c);
2. **Annual seasonality**, modeled using a cosine wave with a one-year period;
3. **Exposure-dependent variation**, through a log-linear relationship where mortality risk increases exponentially with $PM_{2.5}$ concentration.

Mortality counts were simulated independently for each county using actual time series of exposure values, producing a synthetic panel dataset suitable for evaluating causal

estimation methods under known data-generating conditions. In treatment modeling, the daily probability of exposure can be expressed via a dynamic propensity score:

$$e(X_t) = P(T_t = 1 \mid H_t), \quad \text{with} \quad H_t = \left\{\bar{X}_t, \bar{T}_{t-1}, \bar{Y}_{t-1}\right\},$$

where H_t denotes the history of observed exposures, treatments, and outcomes up to time t. In our simulation, we assume strong signal-to-noise ratio for exposure effects, denoted as $\eta_t \gg 0$, to ensure detectable treatment-outcome relationships for evaluation purposes.

Exposure Data. Daily $PM_{2.5}$ exposure levels were obtained from the U.S. High Air Pollutants (USHAP) dataset. For each day, $PM_{2.5}$ estimates were provided at 1-km^2 resolution and aggregated to the county level by spatially overlaying county boundaries. These daily values were used as continuous exposure inputs x_{ct} and further dichotomized into a binary treatment indicator:

$$a_{ct} = \mathbb{1}\{x_{ct} > 11\},$$

where $11\mu g/m^3$ serves as the regulatory threshold commonly used in epidemiological literature and public health standards. All exposure data used in the study were derived from the USHAP files aggregated to 2010 U.S. Census boundaries, consistent with the spatial structure of other county-level covariates. **Potential Confounders.** Several time-varying covariates were included to reflect plausible sources of confounding in environmental health analyses: daily maximum temperature (Tmax), daily precipitation (max), weekday indicator and federal holiday indicator. All covariates were harmonized at the county-day level and aligned temporally with the mortality and exposure data.

Application results and takeaway.

Propensity distributions indicate workable but imperfect overlap; GLM and Super Learner produce similar ranges (Fig. 3). Estimated ATEs (Fig. 4) show a positive contemporaneous effect ($t_{\text{lag}} = 0$) and a smaller positive effect at $t_{\text{lag}} = 1$; CIs exclude zero for $t_{\text{lag}} = 0$ and are borderline at $t_{\text{lag}} = 1$. For $t_{\text{lag}} \geq 2$, point estimates hover near zero with wide intervals, reflecting weaker overlap and accumulated weighting noise. Conclusions: the mortality effect of high $PM_{2.5}$ is short-lived (same-day, possibly next-day), models agree within uncertainty, and inference is driven by overlap/positivity—supporting policies targeting immediate exposure reductions.

8 Discussion

We study duration-t_0 causal effects in single-unit environmental time series and show how time-varying propensity scores $p_t(W_t = 1 \mid \mathcal{F}_t)$ with windowed IPW address feedback, carryover, and seasonality while keeping identification explicit. Practically, define the estimand first; choose $\mathcal{F}_t$ rich enough to block confounding but not so rich that positivity erodes; fit p_t via transparent GLMs or flexible Super Learner with rolling/forward validation to avoid temporal leakage; monitor overlap and weight stability (quantiles, maxima, effective sample size), and use trimming or stabilization if needed. For uncertainty, our martingale variance bound offers conservative, implementation-ready CIs;

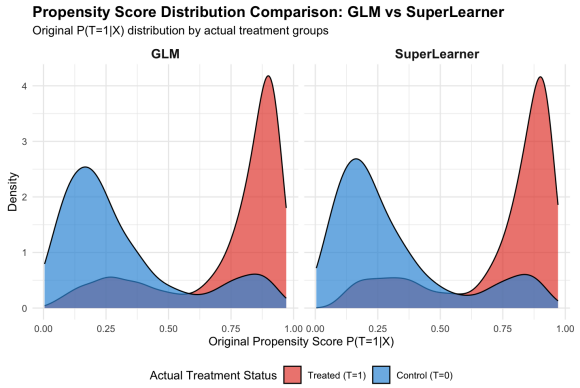

Figure 3: Propensity Score Distribution Comparison from case study ($t_{lag} = 1$)

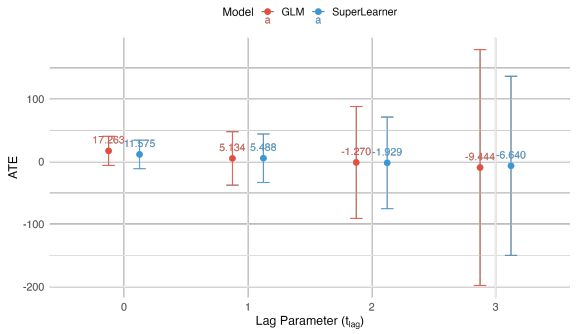

Figure 4: Average Treatment Effect with 95% Confidence Intervel (By lag parameter and model type)

HAC/Newey–West on the influence sequence is a useful sensitivity check. Limitations include the requirement for single-unit, no-interference setting; as well as no-positivity violation assumption and correct PS modeling for the efficiency result. Promising extensions include doubly robust/TMLE estimators, proximal methods for hidden time-varying confounding, explicit treatment of spatial interference, multisite meta-analysis, and policy learning/off-policy evaluation under overlap constraints.

9 Conclusion

We provide a concise framework for observational time-series causal inference in environmental studies: explicit duration-t_0 estimands, a step-by-step IPW estimator using $p_t(W_t = 1 \mid \mathcal{F}_t)$, conservative martingale-bound inference, and an asymptotic result showing that correctly specified estimated propensity scores yield a consistent estimator that is no less efficient than oracle IPW. Simulations and a synthetic California $PM_{2.5}$ analysis demonstrate feasibility, diagnostics, and uncertainty reporting, helping practitioners separate design from analysis and state assumptions transparently; future work will integrate doubly robust learning, spatial interference, and policy learning for dynamic environmental interventions.

References

Bojinov, I.; Rambachan, A.; and Shephard, N. 2021. Panel experiments and dynamic causal effects: A finite population perspective. *Quantitative Economics*, 12(4): 1171–1196.

Bojinov, I.; and Shephard, N. 2019. Time series experiments and causal estimands: exact randomization tests and trading. *Journal of the American Statistical Association*, 114(528): 1665–1682.

Di, Q.; Dai, L.; Wang, Y.; Zanobetti, A.; Choirat, C.; Schwartz, J. D.; and Dominici, F. 2017. Association of short-term exposure to air pollution with mortality in older adults. *Jama*, 318(24): 2446–2456.

Dominici, F.; Peng, R. D.; Bell, M. L.; Pham, L.; McDermott, A.; Zeger, S. L.; and Samet, J. M. 2006. Fine particulate air pollution and hospital admission for cardiovascular and respiratory diseases. *Jama*, 295(10): 1127–1134.

Heyde, C.; and Hall, D. 1980. Martingale limit theory and its applications. *Probability and Mathematical Statistics: A Series of Monographs and Textbooks. Academic Press*.

Kennedy, E. H. 2019. Nonparametric causal effects based on incremental propensity score interventions. *Journal of the American Statistical Association*, 114(526): 645–656.

Lu, Y.; and Zeger, S. L. 2007. On the equivalence of case-crossover and time series methods in environmental epidemiology. *Biostatistics*, 8(2): 337–344.

Papadogeorgou, G.; Imai, K.; Lyall, J.; and Li, F. 2022. Causal inference with spatio-temporal data: Estimating the effects of airstrikes on insurgent violence in Iraq. *Journal of the Royal Statistical Society: Series B (Statistical Methodology)*, 84(5): 1969–1999.

Peng, R. D.; and Dominici, F. 2008. Statistical methods for environmental epidemiology with R. *R: a case study in air pollution and health*.

Rune Christiansen, T. K. M. D. M., Matthias Baumann; and Peters, J. 2022. Toward Causal Inference for Spatio-Temporal Data: Conflict and Forest Loss in Colombia. *Journal of the American Statistical Association*, 117(538): 591–601.

Shahn, Z.; Hernán, M. A.; and Robins, J. M. 2023. A formal causal interpretation of the case-crossover design. *Biometrics*, 79(2): 1330–1343.

Van der Laan, M. J.; Polley, E. C.; and Hubbard, A. E. 2007. Super learner. *Statistical applications in genetics and molecular biology*, 6(1).

Wu, X.; Weinberger, K. R.; Wellenius, G. A.; Dominici, F.; and Braun, D. 2024. Assessing the causal effects of a stochastic intervention in time series data: are heat alerts effective in preventing deaths and hospitalizations? *Biostatistics*, 25(1): 57–79.

A Appendix: Proofs

Proof of Theorem

Proof. (i) For duration t_0 treatment effect, denote the true propensity score $p_t(1|\mathcal{F}_t) = \Pr(W_t = 1|\mathcal{F}_t)$, estimated propensity score $\hat{p}_t(1|\mathcal{F}_t)$ from a correctly specified GLM; and IPW estimator $\hat{\tau}_t^{IPW}(t_0) = w_t(t_0) \times Y_{t+t_0}^{obs}$, where $w_t(t_0) = \prod_{s=t}^{t+t_0} \frac{1}{\hat{p}_s(W_s|\mathcal{F}_s)}$. We make the following assumptions:

1. Correct specification of GLM, i.e., $p_t(1|\mathcal{F}_t) = p_t(1|\mathcal{F}_t;\beta_0)$ for true β_0
2. Positivity: $0 < c \le p_t(1|\mathcal{F}_t) \le 1 - c < 1$ for some $c > 0$
3. Consistency of propensity score estimator, i.e., $\hat{\beta} \xrightarrow{p} \beta_0$ as $T \to \infty$
4. Potential outcome is bounded, i.e., $|Y_t(w_{1:t})| \le M < \infty$.

We can decompose the estimation error

$$\hat{\tau}^{IPW} - \tau = \underbrace{\hat{\tau}^{IPW} - \tau_{true}^{IPW}}_{\text{estimation error of ps}} + \underbrace{\tau_{true}^{IPW} - \tau}_{=0 \text{ by Bojinov Thm 1}}$$

Define the oracle estimator with true propensity scores:

$$\tau_{true}^{IPW} = \frac{1}{T - t_0} \sum_{t=1}^{T-t_0} \frac{(-1)^{1-W_t} Y_t^{obs}}{p_t(W_t|\mathcal{F}_t;\beta_0)}$$

By Theorem 1 in Bojinov 2019, $\mathbb{E}_R[\tau_{true}^{IPW}|\mathcal{F}_{T,t-1}] = \tau$.

Since $\hat{\beta}_T \xrightarrow{p} \beta_0$, the mapping $\beta \mapsto p(1|\mathcal{F}_t;\beta)$ is continuous, and the GLM satisfies regularity conditions (bounded covariates, Lipschitz link function), we have by uniform continuity of the parametric family:

$$\sup_{t,w,\mathcal{F}_t} |\hat{p}_t(w|\mathcal{F}_t) - p_t(w|\mathcal{F}_t)| \xrightarrow{p} 0$$

Therefore by dominated convergence theorem:

$$|\hat{\tau}^{IPW} - \tau_{true}^{IPW}| \le \frac{1}{T - t_0} \sum_{t=1}^{T-t_0} |Y_t^{obs}| \left| \frac{1}{\hat{p}_t(W_t|\mathcal{F}_t)} - \frac{1}{p_t(W_t|\mathcal{F}_t)} \right| \xrightarrow{p} 0$$

Therefore, $\hat{\tau}^{IPW} \xrightarrow{p} \tau$

(ii) Note that estimation error

$$\begin{aligned}
\hat{u}_t &= \frac{(-1)^{1-W_t} Y_t^{obs}}{\hat{p}_t(W_t|\mathcal{F}_t)} - \tau \\
&= \underbrace{\frac{(-1)^{1-W_t} Y_t^{obs}}{p_t(W_t|\mathcal{F}_t)} - \tau}_{u_t \text{(true ps error)}} + \underbrace{(-1)^{1-W_t} Y_t^{obs} \left(\frac{1}{\hat{p}_t(W_t|\mathcal{F}_t)} - \frac{1}{p_t(W_t|\mathcal{F}_t)}\right)}_{\Delta_t \text{(additional error term by using estimated ps)}}
\end{aligned}$$

On the other hand, by first-order Taylor expansion

$$\hat{p}_t(W_t|\mathcal{F}_t) = p_t(W_t|\mathcal{F}_t) + \nabla_\beta p_t(W_t|\mathcal{F}_t;\beta_0)^T \cdot (\hat{\beta}_T - \beta_0) + o_p(||\hat{\beta}_T - \beta_0||)$$

Since $\hat{\beta}_T$ satisfy the score equation $\frac{1}{T}\sum_{s=1}^{T} s_s(\hat{\beta}_T) = 0$ where $s_s(\beta) = \dfrac{\partial \log p_s(W_s|\mathcal{F}_s;\beta)}{\partial \beta}$,

$$\hat{\beta}_T - \beta_0 = -\mathcal{I}_T^{-1} \cdot \frac{1}{T} \sum_{s=1}^{T} s_s(\beta_0) + o_p(1/\sqrt{T}),$$

where $\mathcal{I}_T = -\frac{1}{T}\sum_{s=1}^{T} \dfrac{\partial s_s(\beta_0)}{\partial \beta^T} \xrightarrow{p} \mathcal{I}$.

We note that by Taylor expansion the additional error term can be written as

$$\begin{aligned}
\Delta_t &= (-1)^{1-W_t} Y_t^{obs} \left(\frac{1}{\hat{p}_t(W_t|\mathcal{F}_t)} - \frac{1}{p_t(W_t|\mathcal{F}_t)}\right) \\
&= (-1)^{1-W_t} Y_t^{obs} \cdot \frac{p_t(W_t|\mathcal{F}_t) - \hat{p}_t(W_t|\mathcal{F}_t)}{\hat{p}_t(W_t|\mathcal{F}_t) \cdot p_t(W_t|\mathcal{F}_t)}
\end{aligned}$$

Since we assumed the propensity score model is correctly specified, by the delta method,

$$\Delta_t = \frac{(-1)^{1-W_t} Y_t^{obs}}{p_t^2(W_t|\mathcal{F}_t)} \cdot \nabla_\beta p_t(W_t|\mathcal{F}_t) \cdot (\hat{\beta}_T - \beta_0) + o_p(1/\sqrt{T})$$

We note that since $|Y_t^{obs} \leq M|$ (Assumption 4), $p_t(W_t|\mathcal{F}_t \geq c > 0)$ (Assumption 2), $|\nabla_\beta p_t(W_t|\mathcal{F}_t)| \leq K < \infty$ (regularity of propensity score model), and $\hat{\beta}_T - \beta_0 = O_p(1/\sqrt{T})$,

$$|\Delta|_t \leq \frac{M}{c^2} \cdot K \cdot |\hat{\beta}_T - \beta_0| + o_p(1/\sqrt{T}) = O_p(1/\sqrt{T}),$$

By continuous mapping theorem and Slutsky's theorem, we can decompose the normalized sum S_T as

$$S_T = \frac{1}{\sqrt{T}} \sum_{t=1}^{T-t_0} \hat{u}_t = \frac{1}{\sqrt{T}} \sum_{t=1}^{T-t_0} u_t + \frac{1}{\sqrt{T}} \sum_{t=1}^{T-t_0} \Delta_t.$$

We know from Theorem 3 in Bojinov 2019 that $\mathbb{E}_R[u_t|\mathcal{F}_{T,t-1}] = 0$; Since $\mathbb{E}[\Delta_t|\mathcal{F}_{T,t-1}, \hat{\beta}_T] = O_p(1/\sqrt{T})$ uniformly in $\hat{\beta}_T$, and this rate is integrable, we have:

$$\mathbb{E}[\hat{u}_t|\mathcal{F}_{T,t-1}] = o_p(1/\sqrt{T})$$

Therefore $\{\hat{u}_t, \mathcal{F}_{T,t-1}\}_{t=1}^T$ forms an asymptotic martingale difference array.
To show that the Lindeberg condition holds we need to show that for any $\epsilon > 0$,

$$L_T(\epsilon) = \frac{1}{T-t_0} \sum_{t=1}^{T-t_0} \mathbb{E}_R[\hat{u}_t^2 \cdot \mathbf{1}\{|\hat{u}_t| > \epsilon\sqrt{T-t_0}\}|\mathcal{F}_{T,t-1}] \xrightarrow{p} 0$$

We note that

$$|\hat{u}_t| \leq |\frac{(-1)^{1-W_t} Y_t^{obs}}{\hat{p}_t(W_t|\mathcal{F}_t)}| + |\tau|$$

By Assumptions 2 and 4, and since $\hat{p}_t(W_t|\mathcal{F}_t) \xrightarrow{p} p_t(W_t|\mathcal{F}_t) \geq c > 0$,

$$|\hat{u}_t| \leq \frac{M}{c/2} + |\tau| = C < \infty \text{ w.h.p for large } T$$

Therefore, for $\epsilon > c/\sqrt{T-t_0}$, we have $\mathbf{1}\{|\hat{u}_t| > \epsilon\sqrt{T-t_0}\} = 0$ w.h.p., and as such $L_T(\epsilon) \xrightarrow{p} 0$.
Define conditional variance:

$$\sigma_T^2 := \frac{1}{T-t_0} \sum_{t=1}^{T-t_0} \mathbb{E}_R[\hat{u}_t^2|\mathcal{F}_{T,t-1}]$$

which can be decomposed:

$$\mathbb{E}_R(\hat{u}_t^2|\mathcal{F}_{T,t-1}) = \mathbb{E}_R(u_t^2|\mathcal{F}_{T,t-1}) + \mathbb{E}_R(\Delta_t^2|\mathcal{F}_{T,t-1}) + 2\mathbb{E}_R(u_t, \Delta_t|\mathcal{F}_{T,t-1}).$$

We know from Lemma 1 in Bojinov 2019 that the first term is bounded (i.e., $\mathbb{E}_R(u_t^2|\mathcal{F}_{T,t-1}) \leq \frac{Y_t(w_{1:t}^{obs})^2}{p_t(1)p_t(0)}$), and the last term $\mathbb{E}(\Delta_t^2|\mathcal{F}_{T,t-1}) = O_p(1/T)$ since $\Delta_t = O_p(1/\sqrt{T})$ as shown above.
For the covariance term, we need to evaluate

$$\begin{aligned}\text{Cov}_R(u_t, \Delta_t|\mathcal{F}_{T,t-1}) &= \mathbb{E}_R[u_t \cdot \frac{(-1)^{1-W_t} Y_t^{obs}}{p_t^2} \nabla_\beta p_t^T \cdot \mathcal{I}_T^{-1} \cdot \frac{1}{T} \sum_{s=1}^{T} s_s(\beta_0)|\mathcal{F}_{T,t-1}] \\ &= \frac{1}{T} \sum_{s=1}^{T} \mathbb{E}_R[u_t \cdot \frac{(-1)^{1-W_t} Y_t^{obs}}{p_t^2} \nabla_\beta p_t^T \cdot \mathcal{I}_T^{-1} \cdot s_s(\beta_0)|\mathcal{F}_{T,t-1}]\end{aligned}$$

we note that the cross-terms $\mathbb{E}_R[u_t \cdot s_s(\beta_0)|\mathcal{F}_{T,t-1}]$ for $s \neq t$ vanishes asymptotically:

- For $s < t$: $s_s(\beta_0)$ depends only on $(W_s, \mathcal{F}_s) \subset \mathcal{F}_{T,t-1}$, therefore $s_s(\beta_0)$ is $\mathcal{F}_{T,t-1}$-measurable. In addition, since $\mathcal{I}_T^{-1} \xrightarrow{p} \mathcal{I}^{-1}$; we can show algebraically that

$$\mathbb{E}_R[u_t \cdot \frac{(-1)^{1-W_t} Y_t^{obs}}{p_t^2} \nabla_\beta p_t^T|\mathcal{F}_{T,t-1}] = 0,$$

  we have

$$\mathbb{E}_R[u_t \cdot \frac{(-1)^{1-W_t} Y_t^{obs}}{p_t^2} \nabla_\beta p_t^T \cdot \mathcal{I}_T^{-1} \cdot s_s(\beta_0)|\mathcal{F}_{T,t-1}] = s_s(\beta_0) \cdot \mathcal{I}_T^{-1} \cdot \mathbb{E}_R[u_t \cdot \frac{(-1)^{1-W_t} Y_t^{obs}}{p_t^2} \nabla_\beta p_t^T|\mathcal{F}_{T,t-1}] = 0$$

- For $s > t$: by the tower property,

$$\mathbb{E}_R[u_t \cdot \frac{(-1)^{1-W_t} Y_t^{obs}}{p_t^2} \nabla_\beta p_t^T \cdot \mathcal{I}_T^{-1} \cdot s_s(\beta_0) | \mathcal{F}_{T,t-1}] = \mathbb{E}_R[\mathbb{E}_R[u_t \cdot \frac{(-1)^{1-W_t} Y_t^{obs}}{p_t^2} \nabla_\beta p_t^T \cdot \mathcal{I}_T^{-1} \cdot s_s(\beta_0) | \mathcal{F}_{T,s-1}] | \mathcal{F}_{T,t-1}]$$

  but since all the terms involving t are $\mathcal{F}_{T,s-1}$-measurable when $s > t$ and $\mathbb{E}_R[s_s(\beta_0)|\mathcal{F}_{T,s-1}] = 0$, this expectation is 0 as well.

Therefore, only the $s = t$ term contributes, and thus

$$\begin{aligned}
\text{Cov}_R(u_t, \Delta_t | \mathcal{F}_{T,t-1}) &= \mathbb{E}_R[u_t \cdot \frac{(-1)^{1-W_t} Y_t^{obs}}{p^2(W_t|\mathcal{F}_t)} \nabla_\beta p_t^T (\hat{\beta}_T - \beta_0) | \mathcal{F}_{T,t-1}] \\
&= \mathbb{E}_R[u_t \cdot \frac{(-1)^{1-W_t} Y_t^{obs}}{p_t^2(W_t|\mathcal{F}_t)} \nabla_\beta p_t^T \cdot \mathcal{I}_T^{-1} \cdot \frac{1}{T} \sum_{s=1}^{T} s_s(\beta_0) | \mathcal{F}_{T,t-1}] \\
&= -\frac{1}{T} \mathbb{E}_R[u_t \cdot \frac{(-1)^{1-W_t} Y_t^{obs}}{p_t^2(W_t|\mathcal{F}_t)} \nabla_\beta p_t^T \mathcal{I}^{-1} s_t(\beta_0) | \mathcal{F}_{T,t-1}]
\end{aligned}$$

But $|u_t| \leq M/c + |\tau|$ as shown; $Y_t^{obs} \leq M$ by Assumption 4; $\frac{1}{p_t^2(W_t|\mathcal{F}_t)} \leq \frac{1}{c^2}$ by Assumption 2; $|\nabla_\beta p_t|$, $|\mathcal{I}^{-1}|$ are bounded due to regularity of GLM; and $|s_t(\beta_0) \leq K|$ for some constant K. Therefore

$$|\mathbb{E}_R[u_t \cdot \frac{(-1)^{1-W_t} Y_t^{obs}}{p_t^2(W_t|\mathcal{F}_t)} \nabla_\beta p_t^T \mathcal{I}^{-1} s_t(\beta_0) | \mathcal{F}_{T,t-1}]| \leq B < \infty$$

for some finite constant B, and $|2\mathbb{E}_R[u_t \Delta_t | \mathcal{F}_{T,t-1}]| \leq 2B/T = O(T^{-1})$. Therefore, the conditional variance of $\hat{u}_t$ is bounded for some $\sigma_T^2 \xrightarrow{p} \sigma^2$. As such, since we've already shown that $\hat{u}_t, \mathcal{F}_{T,t}$ is a Martingale difference array and the Lindeberg condition holds, we can apply the Martingale CLT from Hall and Heyde 1980, then

$$\frac{1}{\sqrt{T - t_0}} \sum_{t=1}^{T-t_0} \hat{u}_t \xrightarrow{d} \mathcal{N}(0, \sigma^2), \text{ or equivalently } \sqrt{T - t_0}(\hat{\tau}^{IPW} - \tau) \xrightarrow{d} \mathcal{N}(0, \sigma^2)$$

Finally we calculate σ^2 explicitly to show efficiency. For simplicity write that $V_t = \frac{Y_t^2(1)}{p_t(1|\mathcal{F}_t)} + \frac{Y_t^2(0)}{p_t(0|\mathcal{F}_t)}$. Define $\sigma_{oracle}^2 := \lim_{T \to \infty} \frac{1}{T - t_0} \sum_{t=1}^{T-t_0} V_t$ as the asymptotic variance using true propensity scores. Then,

$$\begin{aligned}
\sigma_T^2 &= \frac{1}{T - t_0} \sum_{t=1}^{T-t_0} \mathbb{E}_R[\hat{u}_t^2 | \mathcal{F}_{T,t-1}] \\
&= \frac{1}{T - t_0} \sum_{t=1}^{T-t_0} [V_t + O_p(T^{-1}) - \frac{2}{T} V_t \cdot \nabla_\beta p_t^T \mathcal{I}^{-1} \nabla_\beta p_t + o(T^{-1})] \\
&= \frac{1}{T - t_0} \sum_{t=1}^{T-t_0} V_t - \frac{2}{T(T - t_0)} \sum_{t=1}^{T-t_0} V_t \cdot \nabla_\beta p_t^T \mathcal{I}^{-1} \nabla_\beta p_t + o_p(1)
\end{aligned}$$

As such,

$$\sigma_T^2 \xrightarrow{p} \sigma^2 = \underbrace{\lim_{T \to \infty} \mathbb{E}_R[\frac{1}{T - t_0} \sum_{t=1}^{T-t_0} V_t]}_{\sigma_{oracle}^2} - \underbrace{\lim_{T \to \infty} \frac{2}{T} \mathbb{E}_R[\frac{1}{T - t_0} \sum_{t=1}^{T-t_0} V_t \cdot \nabla_\beta p_t^T \mathcal{I}^{-1} \nabla_\beta p_t]}_{\text{positive definite}}$$

Since $V_t > 0$ (by non-degenerate potential outcomes and positivity) and $\nabla_\beta p_t^T \mathcal{I}^{-1} \nabla_\beta p_t \geq 0$ (positive semi-definite quadratic form), we have $\sigma^2 \leq \sigma_{oracle}^2$, with equality only when $\nabla_\beta p_t = 0$ a.e. (i.e., propensity score doesn't depend on parameters).

□

B Appendix: Additional Figures and Tables

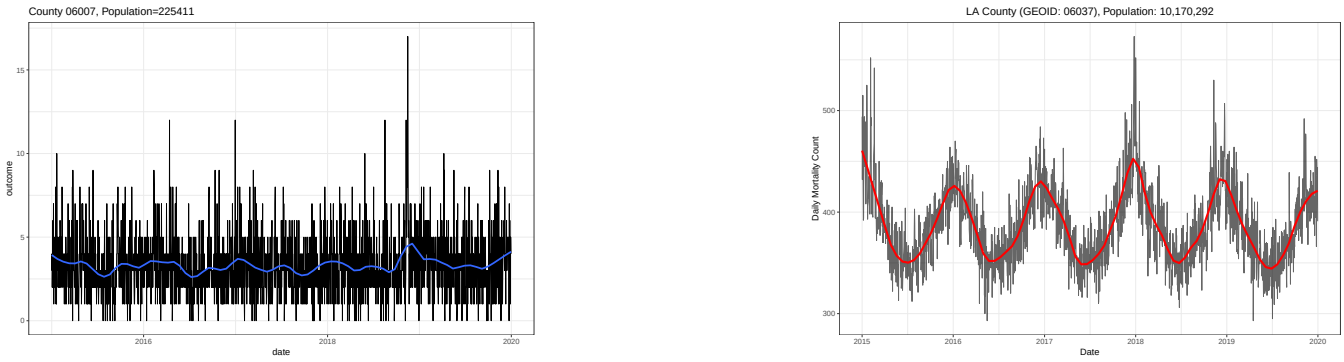

(a) (b)

Figure 5: Synthetic daily mortality time series (2015–2019) for LA County, CA. Black lines show simulated counts; colored curves depict the smoothed seasonal trend.